Laminar structure of the heart: ventricular myocyte arrangement and connective tissue architecture in the dog

I. J. LEGRICE, B. H. SMAILL, L. Z. CHAI, S. G. EDGAR, J. B. GAVIN, AND P. J. HUNTER
Departments of Physiology and Pathology, School of Medicine, and Department of Engineering Science, School of Engineering, University of Auckland, Auckland, New Zealand

LeGrice, I. J., B. H. Smaill, L. Z. Chai, S. G. Edgar, J. B. Gavin, and P. J. Hunter. Laminar structure of the heart: ventricular myocyte arrangement and connective tissue architecture in the dog. *Am. J. Physiol.* 269 (*Heart Circ. Physiol.* 38): H571–H582, 1995.—We have studied the three-dimensional arrangement of ventricular muscle cells and the associated extracellular connective tissue matrix in dog hearts. Four hearts were potassium-arrested, excised, and perfusion-fixed at zero transmural pressure. Full-thickness segments were cut from the right and left ventricular walls at a series of precisely located sites. Morphology was visualized macroscopically and with scanning electron microscopy in *1*) transmural planes of section and *2*) planes tangential to the epicardial surface. The appearance of all specimens was consistent with an ordered laminar arrangement of myocytes with extensive cleavage planes between muscle layers. These planes ran radially from endocardium toward epicardium in transmural section and coincided with the local muscle fiber orientation in tangential section. Stereological techniques were used to quantify aspects of this organization. There was no consistent variation in the cellular organization of muscle layers (48.4 ± 20.4 μm thick and 4 ± 2 myocytes across) transmurally or in different ventricular regions (23 sites in 6 segments), but there was significant transmural variation in the coupling between adjacent layers. The number of branches between layers decreased twofold from subepicardium to midwall, whereas the length distribution of perimysial collagen fibers connecting muscle layers was greatest in the midwall. We conclude that ventricular myocardium is not a uniformly branching continuum but a laminar hierarchy in which it is possible to identify three axes of material symmetry at any point.

ventricular structure; extracellular connective tissue matrix; discrete laminar hierarchy

THE IDEA THAT CARDIAC tissue consists of discrete muscle layers is not new. For several decades, it was accepted that the ventricles were made up of nested muscle bundles, each characterized by a well-defined helical fiber path running from apex to base (11, 12, 15). However, quantitative studies of muscle fiber orientation within the ventricular wall (23, 24) failed to confirm this organization. Ventricular myocardium is now widely viewed as a continuous structure in which muscle fiber orientation varies smoothly through the ventricular walls and which functions as an electrical and mechanical syncitium because of the regular anastomoses between adjacent myocytes. Despite this view, there is convincing evidence for the existence of discontinuity in myocardial architecture at the microscopic and the macroscopic level.

Studies of the extracellular connective tissue matrix in the heart have shown that it has a complex hierarchical organization (2, 4, 16–18). Caulfield and Borg (4) noted that myocytes were connected to adjacent myocytes by a regular array of radial collagen fibers 120–150 nm in diameter. They also reported that a connective tissue meshwork surrounded groups of three or more myocytes and that adjacent bundles of myocytes were loosely coupled by sparse and relatively long collagen fibers. Robinson and co-workers (16–18) categorized further the components of the cardiac extracellular connective tissue network in a series of elegant studies. Most such studies of the cardiac connective tissue matrix focused on aspects of its microstructure, and there has been little attempt to integrate this information with a systematic description of myocyte organization throughout the ventricles. However, there have been reports of large connective tissue septae in the ventricles of the rat (2), macaque (1, 2), dog (2), and human (20). This finding is consistent with macroscopic observations over a number of years. Sections cut from the ventricles of a range of mammalian species reveal extensive extracellular gaps (5–8, 14, 15, 22, 29), and thick longitudinal ventricular sections have a layered appearance due to the numerous cleavage planes that run radially across the wall (5, 7, 8, 22, 29).

It is evident that the three-dimensional arrangement of ventricular myocytes must influence the electrical and mechanical function of the heart. Implicit in most analyses of cardiac function, though, is the assumption that the material properties of the heart are transversely isotropic (9); that is, they are dependent on muscle fiber orientation but independent of direction in the plane transverse to the muscle fiber axis. We believe that this assumption is not consistent with the apparent structural anisotropy of ventricular tissue.

It has been argued elsewhere that the discrete organization of myocytes in ventricular myocardium serves an important mechanical role. The slippage of adjacent muscle layers along the cleavage planes between them is seen to accommodate the substantial changes in ventricular cavity dimension and wall thickness that occur during the cardiac cycle (4, 22). This mechanism has also been invoked to explain aspects of the regional ventricular dilation and local wall thinning that follow myocardial infarction (6, 14, 28). Furthermore it is generally accepted that the extracellular connective tissue matrix is an important determinant of cardiac function and that changes to this network can lead to electrical and mechanical dysfunction in the heart (1, 10, 20, 26, 27). The remodeling of the cardiac extracellular connective tissue hierarchy observed in chronic hypertension (1, 10, 26) and aging (20, 21) has been linked with altered diastolic performance and impaired transverse electrical coupling. Moreover it appears that the connective tissue matrix may be disrupted in acute myocardial ischemia and in "stunned" myocardium (3,

31). It has been argued that this may alter the mechanical properties of the affected regions and contribute to the aberrant wall motion observed under these circumstances.

To understand how the structure of the heart influences its electrical and mechanical function, it is necessary to obtain detailed information about the three-dimensional arrangement of cardiac myocytes and the associated connective tissue hierarchy throughout the walls of right and left ventricles (RV and LV, respectively). Unfortunately, previous observations of the macroscopic organization of cleavage planes in ventricular myocardium have been largely descriptive. As a consequence, perhaps, this potentially important feature of cardiac architecture has not been widely acknowledged in the literature. Moreover there has been no attempt to relate, in any systematic sense, information about spatial arrangement of cardiac myocytes with data on connective tissue organization. The objectives of this study therefore were *1*) to obtain more comprehensive and quantitative information on the cellular architecture of the ventricles and the connective tissue associated with the ventricles and *2*) to quantify the regional variation of important aspects of this structure.

METHODS

Experimental preparation. The methods were approved by the University of Auckland Animal Ethical Committee. Four mongrel dogs weighing 20–33 kg were anesthetized with thiopental sodium (25 mg/kg) and maintained with oxygen and 2% halothane by means of positive-pressure ventilation. A thoracotomy was performed, the pericardium was opened, and a ligature was placed loosely around the ascending aorta. The ligature was tightened as a 50-ml bolus of 15% potassium citrate at 4°C was injected rapidly into the LV via a 14-gauge needle inserted through the apex, causing immediate cardiac arrest.

The heart was rapidly excised and suspended vertically from points around the base in cold (10°C) normal saline. The atria and pulmonary trunk were cut away, and the aorta was transected 20–30 mm above the aortic valve. Left and right coronary arteries were cannulated, and the coronary circulation was flushed with cold cardioplegic solution (13). The heart was then immersed in 3% formaldehyde in phosphate buffer (total osmolarity 850 mosM) while the coronary circulation was perfused with the formaldehyde solution for 30 min at 13 kPa. Because the heart was suspended in a fluid, ventricular transmural pressure was zero and fixation occurred in a well-defined and essentially stress-free state.

To prepare the heart for measurement, a stainless steel spindle was inserted through the fibrous tissue between the mitral and aortic valves and through the apex (the origin of the LV vortex). This formed the longitudinal axis to which geometric data were initially referenced. A circular stainless steel end plate was located on the spindle. Pins were passed through the valve orifices into RV and LV cavities, positioned in radial slots milled in the end plate, and locked in place. Both ventricular cavities were then filled with silicon rubber (Dow Corning, 3110 RTV). The end plate assembly ensured that the heart was firmly located with respect to the spindle, even when parts of the myocardium were later dissected away.

The hearts of two dogs were used to provide a comprehensive description of the gross morphology of the ventricular wall, whereas in two other hearts ventricular architecture was studied using scanning electron microscopy.

Preparation of specimens for macroscopic structural analysis. Ventricular geometry was measured using the specially designed rig previously described by Nielsen et al. (13), which incorporated a vertically mounted probe in a cylindrical polar coordinate system. To make a measurement, axial and angular coordinates were set and the probe was wound down until its tip touched the surface of the heart. This point was determined by the convergence of the tip and its shadow projected by focused side lighting. A laboratory microcomputer was used to evaluate and display the position of the probe tip in cylindrical polar coordinates. Data were stored on operator command.

The RV, interventricular septum, and LV free wall were divided into a series of wedge-shaped segments by means of radial-transmural cuts along meridians spaced at 12° intervals around the heart. Three-dimensional coordinates were recorded along the meridians defining the epicardial and endocardial boundaries of these segments. First, ~500 data points were collected from the meridians on the epicardial surface. The RV free wall was then segmented, leaving the LV intact and the RV cast exposed. Three-dimensional coordinates of the corresponding meridians on the endocardial surface were recorded, and the cast was removed. Next, the RV septal endocardium was mapped out. The LV myocardium was then cut into segments and removed. Finally, endocardial measurements were made on the LV cast.

A series of base-to-apex sections were obtained in two orientations. Frozen sections (100 μm) were cut from equivalent surfaces of each myocardial wedge using a sledge microtome (model Hn40, Reichert Jung) especially adapted for the purpose. This provided a full set of transmural sections at 12° steps around the heart. Each section was floated onto a 120 × 60-mm polycarbonate slide, attached to a background reference grid, and photographed. The section was then allowed to dry for 24 h and rephotographed, the wet and dry records of the section against the background grid being used to check for any shrinkage of the perimeter.

Ten of the myocardial wedges (at 36° spacing) were also sectioned serially through the wall in the plane of the epicardium. The wedge was mounted with the epicardial surface flattened and facing upward. The initial section was a full-length subepicardial surface. Subsequent sections were obtained at 1-mm steps throughout the wall.

Preparation of specimens for scanning electron microscopy. With the heart mounted on the coordinate measurement rig, transmural segments were removed, as shown in Fig. 1, from predetermined LV free wall sites at the anterior equator, lateral base, lateral equator, and posterior apex. The segments were cut parallel to the base of the ventricles, and the coordinates of the epicardial corners were recorded. Typical epicardial dimensions were 20 mm circumferentially and 15 mm in the longitudinal direction. Three to five serial slices, 2 mm thick, were removed from each block. The slices were cut parallel to the epicardial tangent plane with use of a Perspex template and Gem Scientific blades (American Safety Razor, Staunton, VA). Each slice was then carefully trimmed to form a 7.5 × 10 × 2-mm rectangular slab aligned so that the average muscle fiber direction coincided with the short axis of the rectangle. Because the faces of the specimen were near orthogonal to the local muscle fiber axis, they are identified as transverse, tangential, and axial-transmural. The approximate location of each specimen within the slice was recorded, and a fine polyester suture was then drawn through two faces of the specimen to characterize its orientation.

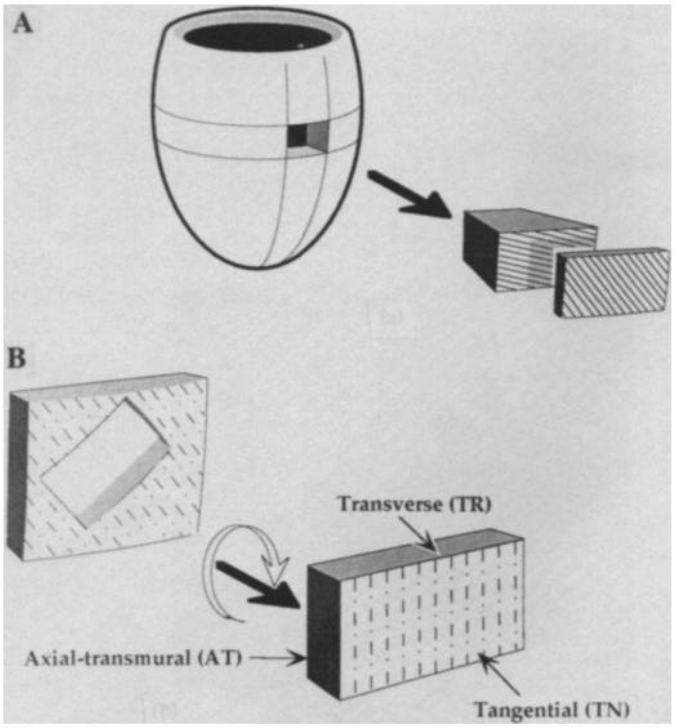

Fig. 1. Schematic diagram of initial steps involved in preparing specimens for scanning electron microscopy. *A*: transmural segment removed from predetermined site in left ventricular wall and divided into 2-mm-thick serial slices. *B*: slices trimmed to 7.5 × 10-mm rectangle, with short axis parallel to mean fiber direction. Orthogonal surfaces are identified as transverse, tangential, and axial-transmural.

A freezing microtome (Cryo-Cut II, Reichert Jung) was used to face off three surfaces on the specimen. A microtome stub was coated with a 1- to 2-mm layer of Tissue-Tek (Miles, Elkhart, IN), an embedding medium for frozen tissue specimens, which was then frozen. This layer was leveled using the microtome, and the inner tangential surface of the specimen was placed on it. An L-shaped polystyrene former with appropriate dimensions was positioned so that it bounded two sides of the specimen. The specimen and former were embedded in Tissue-Tek cooled to −20°C, and the outer tangential surface of the specimen was cut flat with the microtome. Then the specimen composite was removed frozen from the stub and rotated through 90°, and an axial-transmural surface was faced off in the microtome. This process was repeated for the transverse surface of the specimen.

Specimens were stored in phosphate buffer and then dehydrated in a *t*-butanol series (30) and freeze-dried (model ETD4, Edwards) at −60°C for 48 h. They were then mounted on stubs with use of double-sided tape, with the tangential surface closest to the endocardium downward, and were sputter coated with gold (Dynavac mini-coater). A few individual specimens were fractured using a razor blade.

All specimens were viewed using a scanning electron microscope (model DS 130, ISI) at 10–20 kV. The mechanical stage of the microscope provides external control of *x-y* translation of the stub with respect to its axis and complete rotation about the stub axis. In addition, it is possible to rotate the stub axis independently from −10 to +90° with respect to the electron collector. It was therefore possible to view all three faces of the specimen. For each specimen, transverse, tangential, and axial-transmural surfaces were photographed at low magnification (×15–25) to provide registration for subsequent observations at higher power. In some cases, two overlapping micrographs were necessary to record the surfaces completely.

Analysis of macroscopic structure. Digital image analysis was used to quantify the morphology revealed in base-to-apex transmural and circumferential sections. The system consists of a CCD videocamera (model ICD-42E, Ikegame) with a macro zoom lens (Zeiss Tessovar). The camera was connected to an AST 386 personal computer containing a frame grabber board (model PIP-1024A, MATROX Electronic Systems).

Muscle layer orientations were recorded from 30 transverse sections equally spaced around the heart, and ~550 observations were made on each section. At each observation point, a short vector was drawn parallel to the local sheet direction with use of the computer mouse, and the cylindrical polar coordinates of the point were recorded along with the vector orientation. The camera-and-lens system limited the maximum area of section imaged at one time to a 15 × 10-mm rectangle; thus it was necessary to process several separate images to cover the whole section.

To characterize the organization of branches between adjacent layers, the edges of layers were identified in digitized video images of selected areas in longitudinal-circumferential and longitudinal-transmural sections. Muscle layers were traced, using the computer mouse, in a sampling area 5 mm deep in the longitudinal direction and occupying the full width of the section. Gray-scale records of the composite video image were then printed. Six representative "equatorial" regions were studied in one dog heart: one each in the anterior and posterior LV free wall, the lateral RV free wall, and the interventricular septum and two in the lateral LV free wall. For each of these regions, muscle layer boundaries in corresponding sample areas were traced in a series of longitudinal-circumferential sections spaced at 2-mm intervals through the wall in the LV and at 1-mm intervals in the RV. Records were also collected from matching longitudinal-transmural sections at sites adjacent to the areas sampled in the circumferential sections.

We used two measures of the branching between muscle layers: *1*) the number of branches per unit area was determined for each sampling area, and *2*) relative path length was also estimated. The relative path length is the distance that it is necessary to move along muscle layers in order to traverse a given distance perpendicular to the layers.

Morphological analysis of scanning electron microscopy. Two to three regions were selected from the low-power micrographs of the tangential and transverse surfaces. Areas in which structure was clearly resolved were chosen randomly and viewed with the scanning electron microscope. Further micrographs were obtained at ×75 for transverse surfaces and ×50 for tangential surfaces and enlarged photographically to A4 size (30 × 21 cm).

For the transverse surface, we estimated *1*) the volume fraction occupied by myocytes and *2*) the lengths of perimysial connective tissue fibers connecting adjacent muscle layers. To estimate volume fractions of myocardial components, a transparent counting matrix with 31 × 21 fine dots on a 5-mm grid was placed over the transverse micrographs, and the numbers of dots falling on myocytes were recorded. The location of the grid on the micrograph was noted, and the process was repeated with the grid at a different site. Finally, the lengths of perimysial connective tissue fibers connecting adjacent muscle layers were recorded only if both ends could be observed and there was no evidence of perimysial disruption. Between 20 and 30 measurements of fiber length were made for each micrograph, and the regions thus analyzed were also carefully recorded.

Similar methods were used to quantify structure in micrographs of tangential surfaces. In this case, we estimated *1*) the numbers of cells in different muscle layers, *2*) the average transverse dimension of muscle layers, and *3*) the number of branches between adjacent layers per unit surface area. An A4 transparency with 13 horizontal lines spaced 15 mm apart was placed over the micrograph so that the lines were perpendicular to the local orientation of the muscle layers. Regions in which the edges of the muscle layers and the boundaries of myocytes were clearly resolved were selected, and their locations were recorded. The numbers of layers and the number of cells within layers were counted along each line, and the width of the layers was also estimated. The number of branches between adjacent layers was also counted within selected areas in each micrograph.

Statistical analysis. For morphological indexes derived from serial specimens for a given ventricular region, a one-way analysis of variance was used to assess the extent of their transmural variation. Unless otherwise stated, values are means ± SD.

RESULTS

Gross morphology. There was little change in the boundary dimensions of the thick longitudinal-transmural and longitudinal-circumferential specimens during processing. However, the tissue shrinkage within the specimens due to dehydration was 15–20%, which made the laminar organization more evident.

All thick longitudinal-transmural sections had a similar appearance. The LV anterior free wall section presented in Fig. 2*A* reveals an array of discrete tissue layers that run across the ventricular wall from endocardium to epicardium in an approximately radial direction. Whereas there is extensive branching of muscle layers throughout the section, the radial extent of the gaps between adjacent layers is striking, i.e., up to 4 or 5 mm in the midwall. Closer inspection reveals a somewhat more uniformly coupled structure in subepicardial and subendocardial regions. In the equatorial region, the laminated appearance is less evident at some sites and two distinct layer orientations can be identified.

In the longitudinal-circumferential sections (Fig. 2*B*), muscle layers coincide with the local muscle fiber direction. The progressive change in the apparent orientation of layers in the successive serial sections is consistent with the known transmural variation of fiber angle.

A schematic diagram of transverse sheet organization is given in Fig. 3. At the center is a plan view of the heart, with short radial lines representing the locations of the transverse-axial sections studied. Observations for sections with similar surface geometry and sheet orientation have been grouped, and, on this basis, the myocardium was subdivided into the seven regions indicated. The widely spaced radial lines represent myocardial layer orientation, whereas the denser shading indicates trabeculae or papillary muscle. All sections are viewed with the LV lumen to the left.

Figure 4 provides a more quantitative representation of the results in Fig. 3. The transmural variation of muscle layer orientation in transverse-axial section is given for representative sites through LV free wall, interventricular septum, and RV free wall. All angles were measured relative to the local outer-wall surface

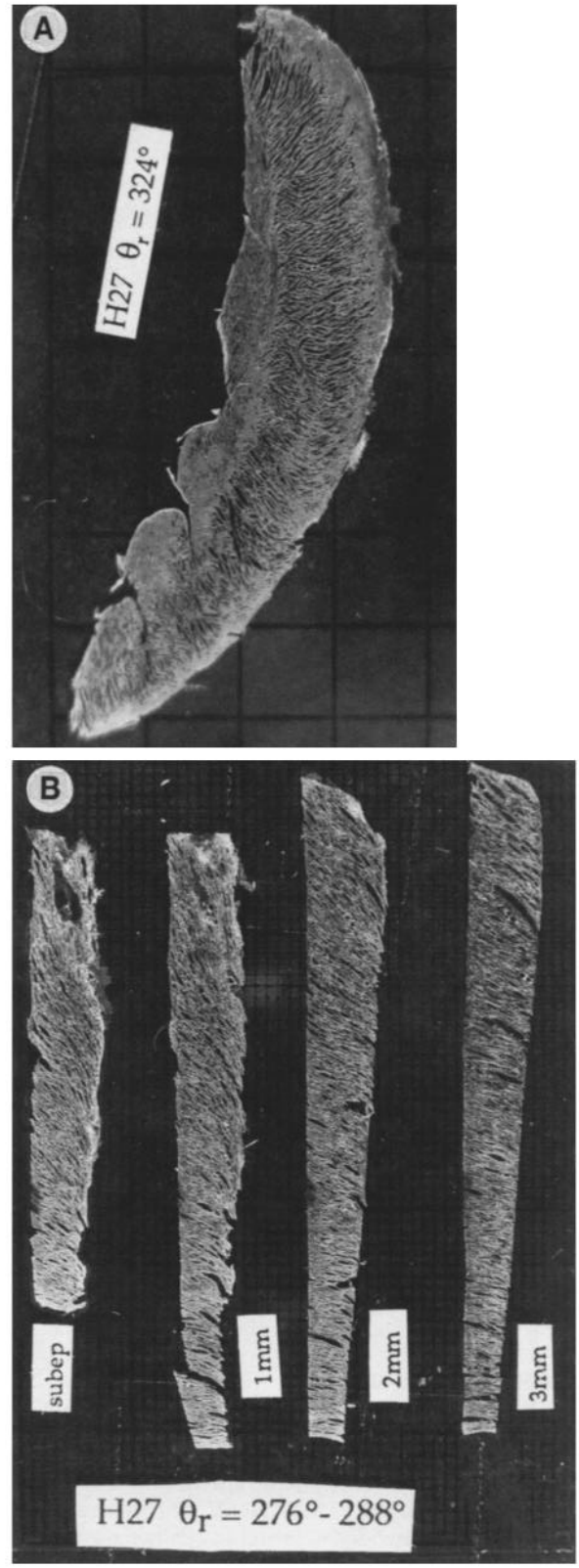

Fig. 2. *A*: micrograph of longitudinal-transmural section of left ventricle showing typical radial alignment of myocyte layers. *B*: sequence of micrographs in longitudinal-circumferential section showing layered organization with transmural variation of fiber angle. H27, heart 27; θ_r, circumferential coordinate; subep, subepicardium.

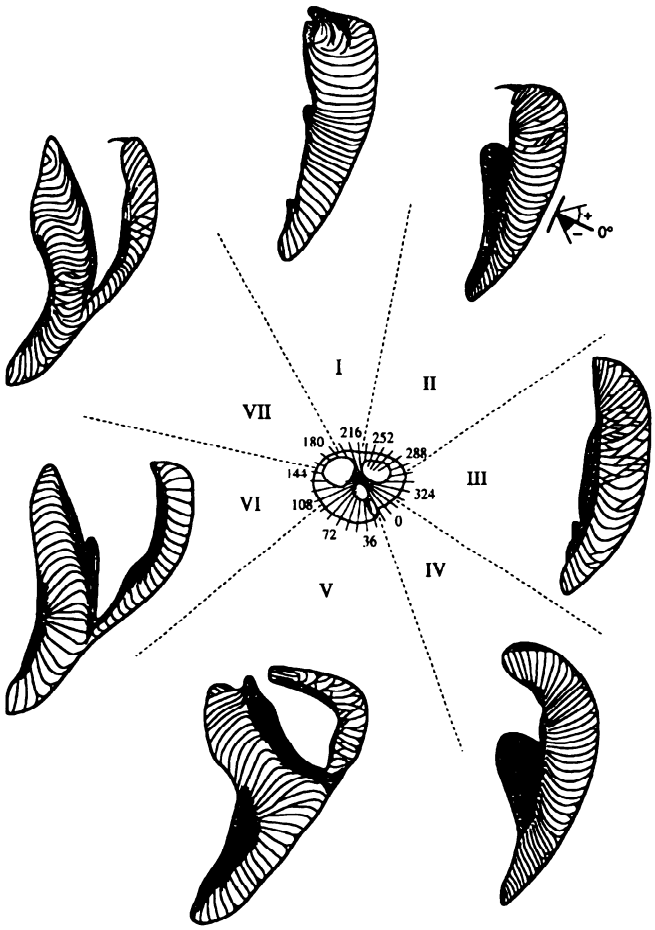

Fig. 3. Longitudinal-transmural sections of ventricles from a series of circumferential locations. Orientations of myocardial laminae are shown for each section (sketched from original data).

normal, as shown in Fig. 3. The mean muscle layer angle at each point is obtained by pooling measurements from sample volumes immediately adjacent to the point. The transmural variation of muscle layer orientation at the equator is similar for LV and RV free walls, with layer orientation progressively changing from around −90° at the endocardium to 30–60° at the epicardium. For the interventricular septum, however, the transmural variation of muscle layer orientation at the equator is opposite in sense, changing from 90° in the LV subendocardium to around −90° in the RV subendocardium.

Figure 5*A* shows the density of branches estimated from longitudinal-circumferential sections at the four LV sites. Depths are normalized for wall thickness excluding endocardial structures such as trabeculae or papillary muscle, and a depth of zero represents the transition from normal myocardium to trabecular or papillary muscle. At each site, there is a similar transmural variation, with higher branching densities for subepicardial and subendocardial sections and a minimum near midwall. On average, there are 8.4 branches/mm^2 in subepicardial sections, decreasing to a minimum of 3.8 in the midwall and then rising to 6.6 in subendocardial sections. Relative path lengths for the four LV sites are shown in Fig. 5*B*. The mean relative path length at the subepicardium is 1.9, increasing to an average maximum of 3.1 near midwall and returning to 1.9 for the subendocardium. Similar results for branching density and estimated path length were obtained for RV and septal sites. Estimates of branching frequency obtained for longitudinal-transmural thick sections were typically less than those from corresponding longitudinal-circumferential sections.

Microscopic structure. Laminar structure was evident in each of the specimens viewed with the scanning electron microscope. Figure 6*A* is a micrograph from a typical specimen oriented so that all three orthogonal faces could be observed at the same time. This specimen

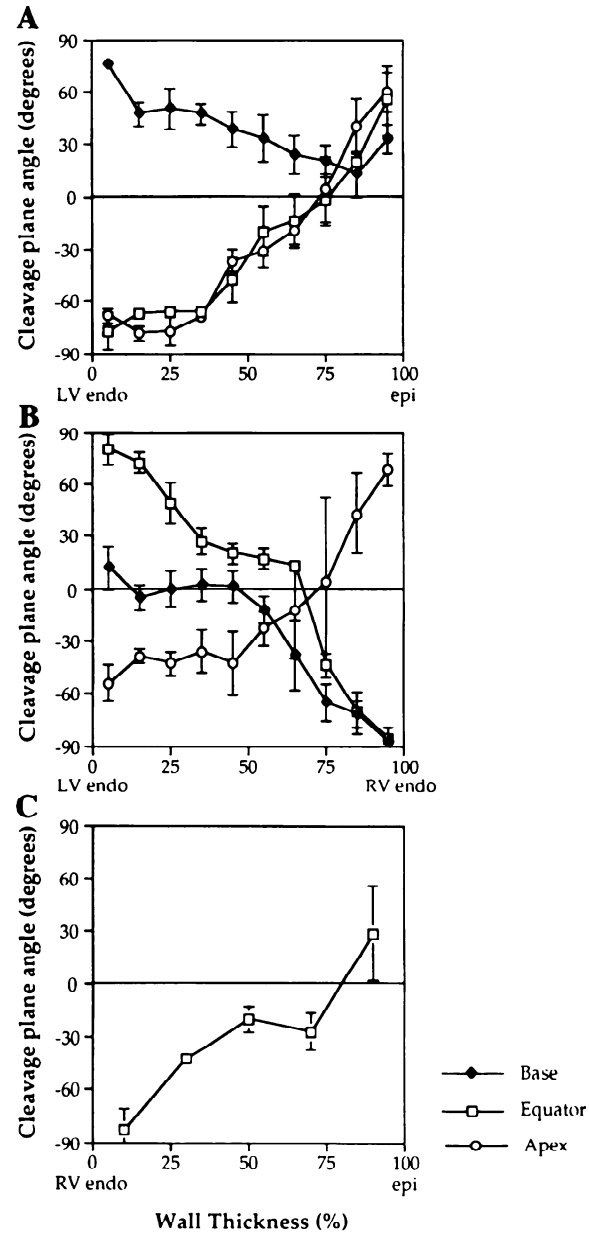

Fig. 4. Transmural variation of muscle layer orientation in selected longitudinal-transmural sections: left ventricle (LV) (*region II, A*), septum (*region VI, B*), and right ventricle (RV) (*region VI, C*). Locations of sections correspond to regions defined in Fig. 3. Angles were measured relative to outer-wall normal (Fig. 3, *sector II*). Local surface normal represents 0°, and anticlockwise angles are positive. Data from 3 longitudinal sites are shown for left ventricle and septum and one for right ventricle.

was cut below the subepicardium from a midanterior LV transmural block. The laminated appearance of myocardium is most clearly seen in tangential section (Fig. 6*B*). In this view, we consistently observed an organization that resembled an array of stacked layers or sheets. Branching between adjacent layers is relatively sparse, and the distance along any sheet between two such branches can be 1–2 mm. Closer observation of the layers shows that they consist of tightly packed groups of cardiac myocytes aligned so that the cell axis is approximately parallel to the cut edge of the layer. At this level, the layers appear to be uniform in structure, with regular anastomoses between adjacent cells and an ordered interdigitation of cells and capillaries. Typically, there are four myocytes across the thickness of a layer, whereas branches between adjacent layers are generally one to two myocytes thick. In those areas where there are appreciable spaces between adjacent layers, their radial extent appears to be considerable and an extensive network of connective tissue is observed. Long collagen fibers run between muscle layers and insert into the connective tissue network that surrounds them

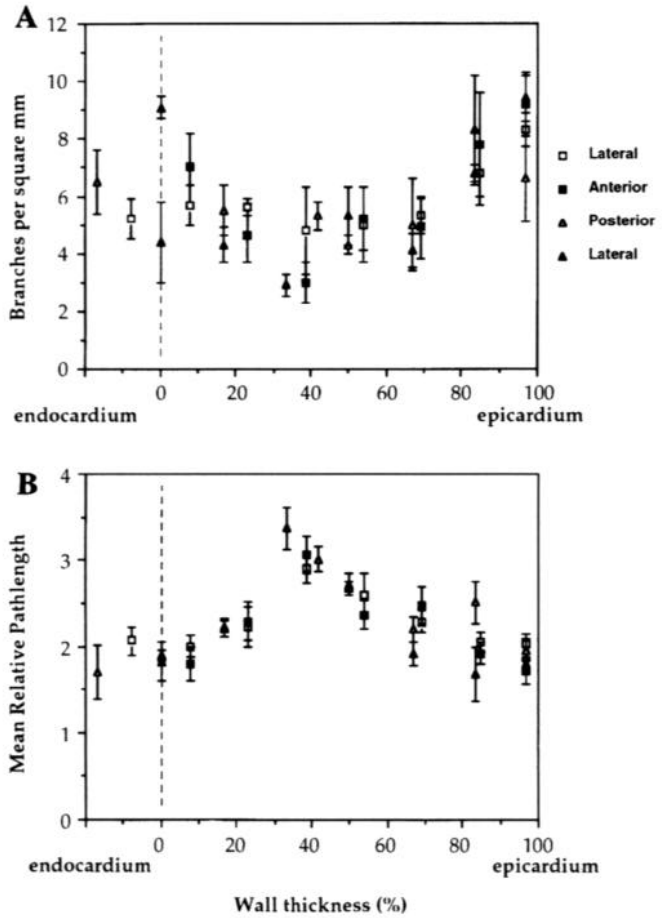

Fig. 5. Transmural variation in sheet branching for left ventricular myocardium in longitudinal-circumferential plane. *A*: sheet-to-sheet branching density recorded from 100-μm apex-to-base sections at anterior, lateral, and posterior equatorial sites in left ventricular free wall. *B*: transmural variation in sheet center line path length for a perpendicular crossing of a series of sheets. Path length is normalized relative to direct perpendicular distance across sheets. At *left* of dashed lines is trabecular or papillary muscle tissue.

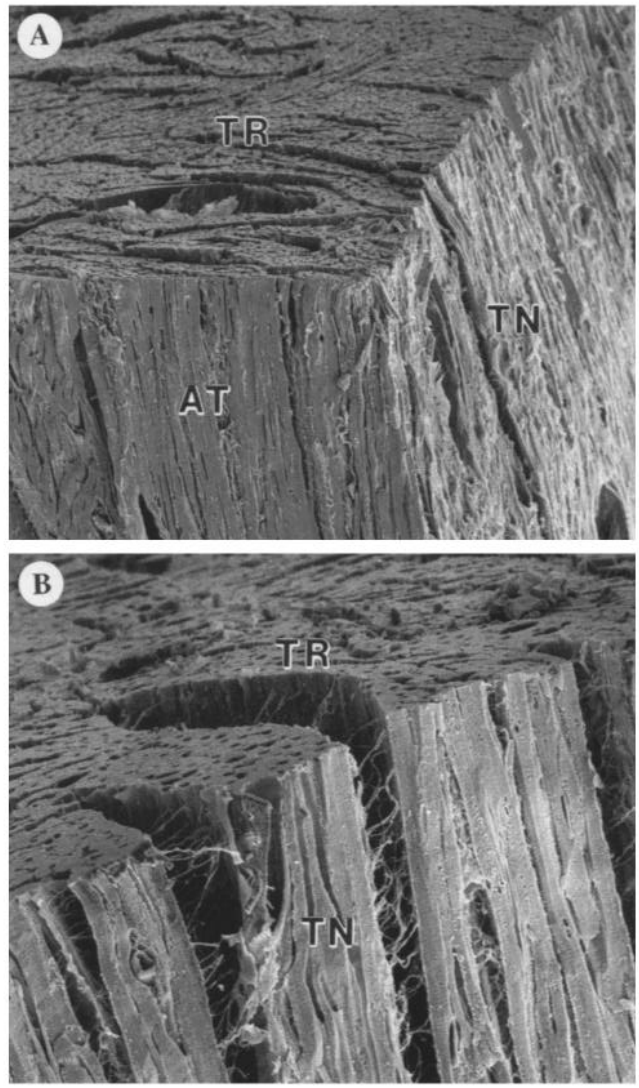

Fig. 6. Scanning electron micrographs showing 3 orthogonal surfaces of a typical left ventricular midanterior midwall specimen. *A*: oblique view of tangential (TN), axial-transmural (AT), and transverse (TR) faces of specimen. *B*: view of TN and TR surfaces.

(Fig. 7). These perimysial collagen fibers connect adjacent muscle layers and should not be confused with the thicker coiled perimysial fibers (18) that run approximately parallel to the myocyte fiber axis.

Layered structure was also apparent in the transverse surface of our specimens (Fig. 8). Again, myocytes are organized in groups three to four cells deep, and there is some branching between adjacent layers. However, in many cases, branching is relatively infrequent and the radial extent of the gaps between sheets can be considerable. The extensive network of connective tissue that surrounds the myocardial layers can be readily observed in this plane. Finally, the density and uniform distribution of capillaries are particularly striking in transverse section. It is noteworthy also that pre- and postcapillary vessels were generally observed within layers and not in the cleavage planes that separate them.

The number of myocytes through the thickness of individual muscle layers was estimated from the tangen-

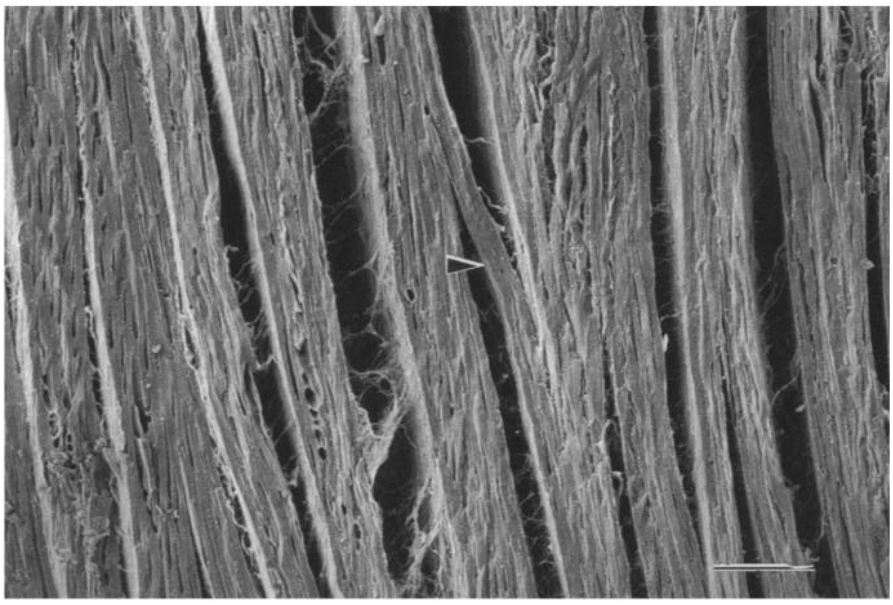

Fig. 7. Micrograph of tangential surface of specimen showing layered organization of myocytes, branching of layers (arrow), and collagen fibers between adjacent sheets. Scale bar, 100 μm.

tial surface of the specimens studied. The mean number of myocytes per layer was very similar in all cases, with a minimum of 3.4 myocytes/layer and a maximum of 4.4. Figure 9 gives the distributions of myocytes per layer obtained from a series of four specimens cut from an individual LV basolateral block. The number of cells observed through a muscle layer varied from 1 to 12, and similar distributions were seen at all transmural sites. These data coincide with the observation that there were typically four myocytes across a layer. However, muscle branches between adjacent layers were one to two cells thick, whereas some double bundles, seven to eight cells thick, were also seen. Transmural data for all segments are superimposed in Fig. 10, and analysis of variance revealed no significant transmural variation in the number of myocytes per layer. Layer thickness was 48.4 ± 20.4 μm. There was no consistent transmural variation in layer thickness; nor was there any significant difference in the data for different ventricular regions.

In Fig. 11*A*, we present estimates of the volume fraction occupied by myocytes in transverse surfaces at different sites through the LV wall for the six blocks studied. We give corresponding results for the estimated length of the perimysial fibers connecting adjacent muscle layers and the density of muscle branches between neighboring layers in Fig. 11, *B* and *C*, respectively.

In all three cases, there is a significant transmural variation in the data (Table 1) but no difference in the results for different ventricular sites. The relative proportion of extracellular space increased progressively from the subepicardium to the deep midwall, indicating that muscle layers are most tightly coupled in the subepicardium. The length of perimysial fibers connecting adjacent muscle layers also increased progressively through

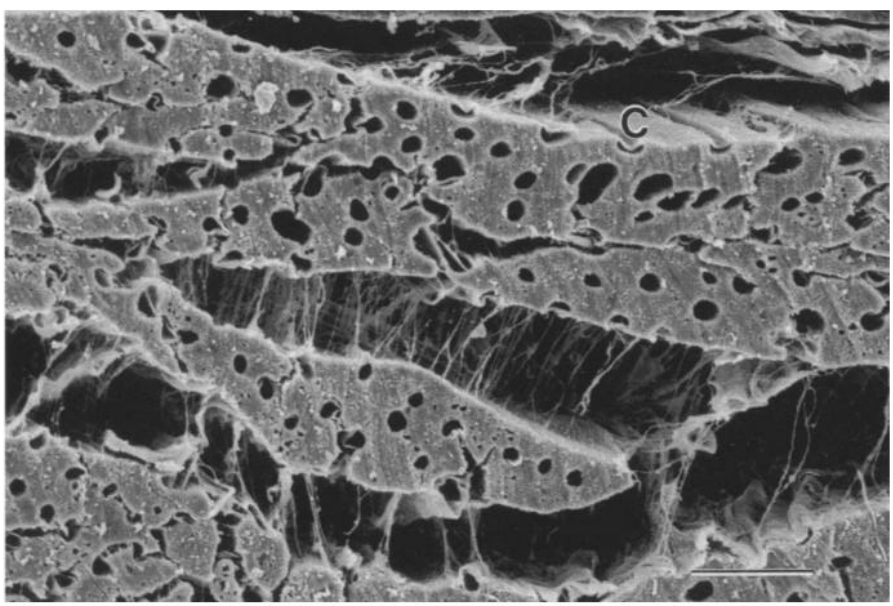

Fig. 8. Micrograph of transverse surface of specimen. Perimysial connective tissue weave surrounding myocardial sheets is evident and covers surface capillaries (C). Scale bar, 25 μm.

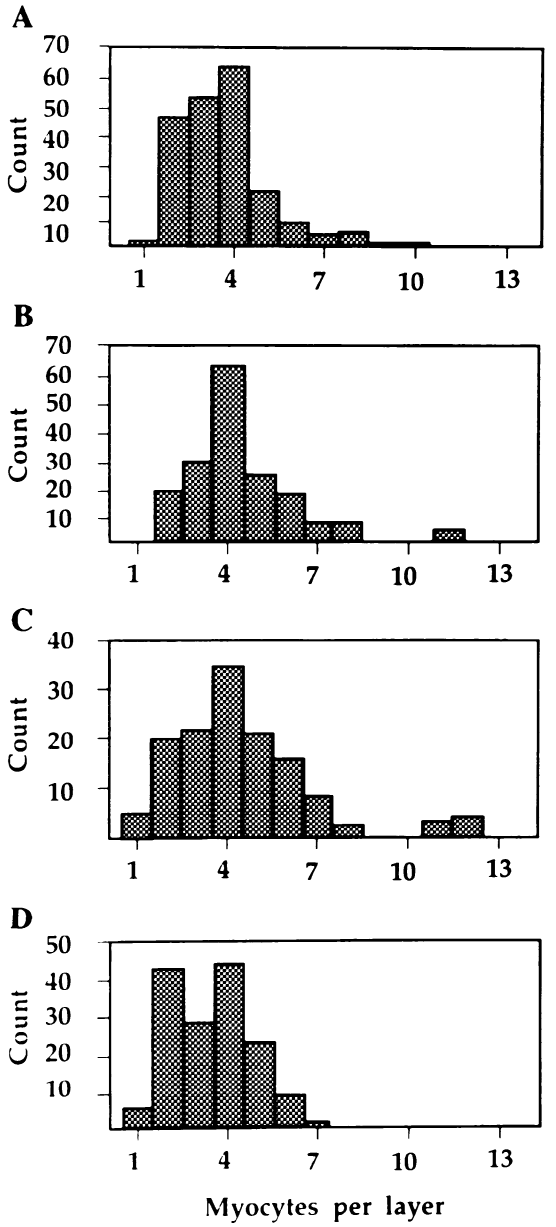

Fig. 9. Distributions of myocytes per layer at different sites through left ventricular wall at lateral base (*block 1.2*). *A*: subepicardium; *B–D*: serial sites through to deep midwall.

the ventricular wall. The mean length of perimysial fibers connecting adjacent layers in the subepicardium varied from 13.2 to 19.8 μm but ranged from 22.3 to 49.4 μm in the deep midwall. Moreover the length distribution of these perimysial fibers is considerably wider for the midwall than for the subepicardium. Finally, the number of longitudinal branches between adjacent muscle layers was considerably greater in the subepicardium than in the midwall of the LV. The mean number of branches per square millimeter in the subepicardium varied from 11.96 to 15.08, but in the deep midwall the comparable values were 4.91–7.84.

DISCUSSION

This study indicates that ventricular myocardium is not a uniformly connected structure but is instead a hierarchy of discrete muscle layers that have a characteristic three-dimensional organization. We have investigated this laminar architecture macroscopically and with scanning electron microscopy and have also quantified aspects of its arrangement.

The laminar organization of the ventricles is evident at a relatively macroscopic level. The cut edges of layers are parallel with the muscle fiber axis in tangential section, but in apex-base transmural sections the boundaries of the layers follow a curving radial path from subendocardium to subepicardium. Systematic observation of the transmural sections reveals subtle variations in the local orientation of muscle layers for different ventricular regions, and these patterns appear to be repeated in different hearts. The radial and tangential extent of individual layers is surprisingly large, and branching between adjacent layers is relatively sparse, particularly in the midwall of the LV.

The organization of myocytes within layers conforms closely with the accepted view of cardiac cellular organization. A typical muscle layer consists of a uniformly connected array of myocytes stacked four cells deep. Branches connecting adjacent layers are one to two cells thick, and aggregates of two or more layers were observed in some cases. The distributions of the number of myocytes observed through the thickness of a layer were highly consistent, and no systematic transmural variation was observed in these data when results for all regions were pooled.

Despite the uniformity of muscle layer organization, the architecture of ventricular myocardium is not homogeneous. There is a clear transmural variation in the extent of coupling between adjacent layers, with a progressive reduction in the estimated density of branching between adjacent muscle layers from the subepicardium through to the deep midwall. Likewise, there is a considerable difference in the lengths of the perimysial collagen fibers that connect adjacent muscle layers at different sites through the LV wall. In the subepicardium, the interconnecting perimysial fibers range in

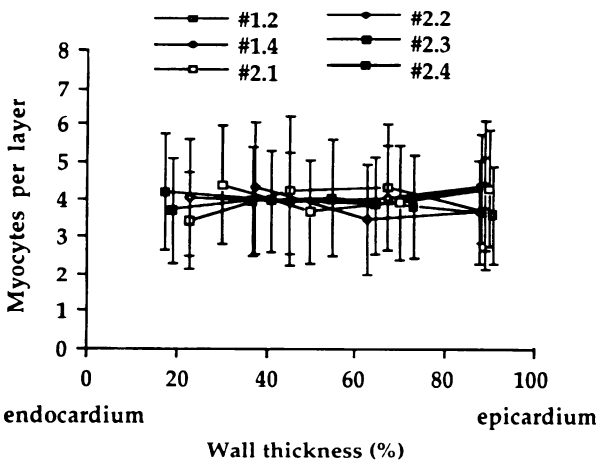

Fig. 10. Myocytes per layer at different sites through left ventricular wall. Transmural data are presented for anterior equator (*block 2.1*), lateral base (*blocks 1.2* and *2.2*), lateral equator (*block 2.3*), and posterior apex (*blocks 1.4* and *2.4*).

length from 6 to 30 μm, whereas in the deep midwall the distribution of lengths is much wider.

The observations reported are to some extent facilitated by methods used in the study. Light-microscopic comparison with fresh unfixed ventricular tissue indicates that myocyte dimensions are slightly reduced by fixation and processing for electron microscopy, whereas the space between muscle layers is expanded. Although cleavage planes can be observed in fresh myocardial tissue at a magnification of ×10–20, they are more clearly revealed in processed specimens. Scanning electron microscopy provides no evidence that laminar architecture is altered or that the associated extracellular connective tissue network is grossly disrupted by fixation or processing. When specimens are prepared for macroscopic observation, the thick sections of myocardium are dehydrated, which results in the shrinkage of some tissue components and further accentuates the gaps between layers. Careful comparison of sections before and after they were dried demonstrates that the radial orientation of layers is not significantly altered. Moreover, connections between adjacent layers appear to be preserved.

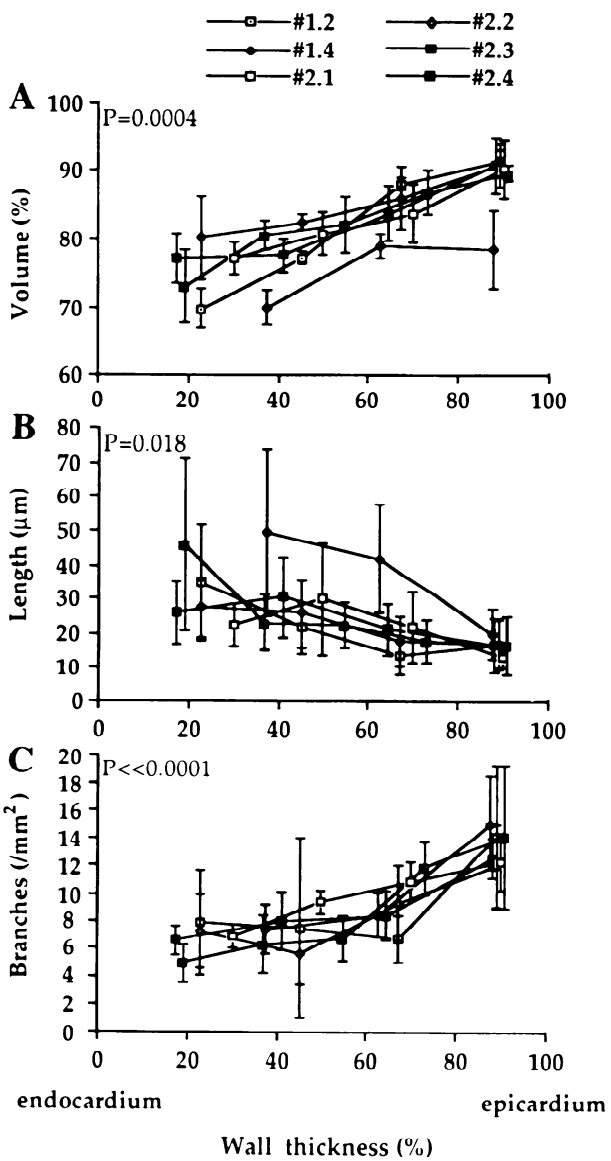

Fig. 11. Volume fraction of myocytes (*A*), length of perimysial fibers connecting adjacent layers (*B*), and numbers of branches between adjacent layers at different sites through left ventricular wall (*C*). Transmural data are presented for anterior equator (*block 2.1*), lateral base (*blocks 1.2* and *2.2*), lateral equator (*block 2.3*), and posterior apex (*blocks 1.4* and *2.4*). *P* values are for 1-way analysis of variance.

Table 1. *Volume fraction of myocytes, length of perimysial fibers connecting adjacent layers, and numbers of branches between adjacent layers at different sites through left ventricular wall*

	Inner Wall	Midwall	Outer Wall	*P*
Volume, %	75 ± 4	81 ± 5	88 ± 5	0.0004
Length, μm	31 ± 9	27 ± 10	17 ± 3	0.018
Branches, mm^{-2}	6.7 ± 1.1	7.6 ± 1.2	12.8 ± 1.4	≪ 0.0001

Values (means ± SD) are from data in Fig. 11 for inner wall (0–33% depth), midwall (34–66%), and outer wall (67–100%). *P* values are for 1-way analysis of variance.

The methods used in this study provide a systematic and quantitative basis for characterizing aspects of the cellular architecture of myocardium. Detailed measurements of muscle layer orientation have been made in serial base-apex sections and accurately referred to ventricular geometry. This has provided comprehensive data on the macroscopic arrangement of cleavage planes within the ventricles. In reconstructing myocardial organization from scanning electron micrographs, the technique of sectioning and observing three orthogonal surfaces in each specimen has proved invaluable. This method inherently provides a more precise spatial registration of structure and also gives a basis for systematic observation of the various elements of the structural hierarchy. Strenuous efforts were made to identify accurately the location of all specimens in relation to the measured ventricular geometry and to standardize the orientation of sections with respect to the muscle fiber axis. Care was also taken to minimize bias in the selection of regions for quantitative analysis. Two to three separate regions were studied for the longitudinal-tangential and transverse faces of each specimen, and analytic procedures involved exhaustive and repeated observation. Finally, analysis procedures were designed so that the complete process could be reproduced or extended at any stage.

A number of errors are inherent in the methods used in this study. Individual muscle layers could not easily be resolved by macroscopic observation, which introduced uncertainty when the frequency of branching between adjacent layers was estimated. In quantifying features revealed in scanning electron micrographs, absolute dimensions are incorrectly estimated due to *1*) shrinkage, *2*) imperfect alignment of sections with respect to the muscle fiber axis, and *3*) the fact that structures, such as the perimysial collagen fibers connecting adjacent muscle layers, may be obliquely oriented with respect to the plane of section. Uncertainty is also introduced in the normalized volume fraction estimates when structures of interest are obscured in the thick sections studied. This can occur if the sample is inappro-

priately oriented within the scanning electron microscope or when, as sometimes happened, the sample attached to the stub deforms during processing. Such errors were minimized by aligning the sample so that the region of interest was, as far as possible, transverse to the electron beam.

Despite these reservations, the results were acceptably repeatable. In all cases, comparable data from the specimens studied using scanning electron microscopy were consistent, and there appears to be no systematic difference in the results for the separate regions studied. The transmural variation of morphological indexes that reflect the extent of coupling between muscle layers is particularly striking when data from all studies are pooled. Finally, the macroscopic and scanning electron microscopic studies yielded similar results for the magnitude and variation of the frequency of branching between adjacent muscle layers at different sites through the LV wall.

The results presented here are consistent with previous observations (5–8, 22, 29) that ventricular myocardium is a composite of muscle layers that run radially across the ventricular wall from subendocardium to subepicardium. We have provided a more detailed and more systematic account of the architecture of these sheets. In doing this, we have identified no major component of the connective tissue hierarchy not already described by Caulfield and Borg (4) and Robinson et al. (16). It is evident that the layers observed in this study may be equated with the "bundles" of myocytes reported by these workers, but they did not recognize the extensiveness of the discrete muscle layers in ventricular myocardium. In fact, Robinson et al. (16, 17) placed the most emphasis on connective tissue architecture in papillary muscle in which the cellular organization corresponds relatively closely with that of skeletal muscle. The organization of papillary muscle differs considerably from that of ventricular myocardium and is not an appropriate model of ventricular structure.

In reconstructing the three-dimensional architecture of ventricular myocardium, it is necessary to reconcile the continuous variation of muscle fiber orientation through the wall of the heart with the observed transmural organization of muscle layers. The schematic in Fig. 12 extends ideas proposed by Feneis (5) and provides a simple structural model that gives some insight into this problem. Muscle layers are represented as transmural sheets twisted to accommodate local muscle fiber orientation. It is evident that the axial extent of a single sheet must be limited. Hence, branches between adjacent muscle layers would play an important role in the assembly of such a structure. It should not be imagined that the three-dimensional organization of muscle layers illustrated in Fig. 12 is the only possible arrangement: within such a hierarchy of muscle layers a range of various transmural connections is possible.

The extent to which the three-dimensional organization of structure such as this can be inferred from a restricted set of two-dimensional projections is inevitably limited. A more powerful approach would be to employ established volume reconstruction and analysis methods with use of an imaging modality such as

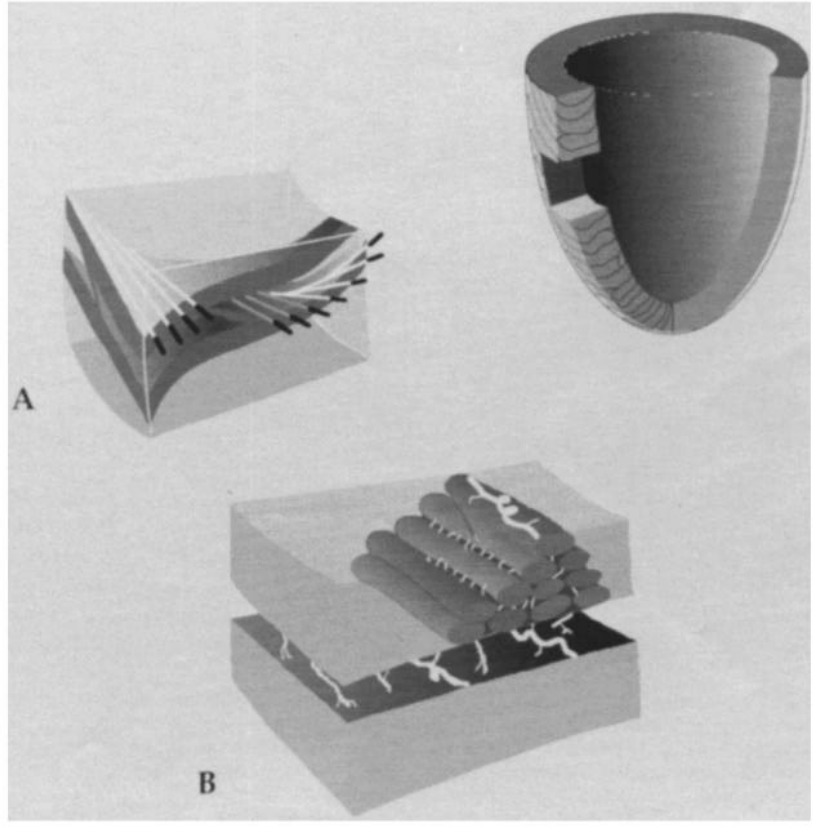

Fig. 12. Schematic of cardiac microstructure. Transmural segment (*A, left*) contains layers of tightly coupled myocytes. These layers run in an approximately radial direction, and there are circumferential and tangential muscle branches between adjacent layers. Orientations of muscle fiber axes are indicated. *B*: cellular arrangement. Fine lines, components of extracellular collagen matrix.

confocal laser microscopy. This should provide more accurate measurements of morphology and a better understanding of three-dimensional arrangement of muscle layers. Studies along these lines are now well advanced in our laboratory.

Our results support the contention that cleavage planes in the ventricular wall permit the rearrangement of muscle fiber bundles when wall thickness changes. Feneis (5), Hort (7), and Grimm et al. (6) argued that this structure would support lateral movement or shear of muscle layers with respect to each other. This mechanism has also been used to explain regional changes in ventricular dimension associated with myocardial infarction (14, 28). Spotnitz et al. (22) demonstrated that the orientation of cleavage planes within the ventricular wall became progressively more oblique as ventricular volume was increased and wall thinning occurred. According to Waldman, Fung, and Covell (25), the patterns of wall thickening and longitudinal-radial shear observed in studies of regional three-dimensional deformation in the beating dog heart indicate a greater degree of mechanical coupling through the ventricular wall than has generally been acknowledged. It is possible that the laminar architecture of the myocardium and the transmural variation of coupling between layers provide a framework that enables muscle fiber extension and wall stress to be appropriately distributed through the ventricular wall during systole and diastole (19).

The laminar organization of ventricular myocardium may also affect the propagation of cardiac electrical activation, and this point has been raised in an associated context by Spach and co-workers (20, 21). If it is assumed that muscle layers are electrically insulated, depolarization can spread to adjacent laminae only via direct muscle branches. Therefore the path required to traverse a given distance perpendicular to the layers will be convoluted, particularly in the midventricular wall, where the frequency of branching is relatively low. On the basis of our estimates of relative path length, we would expect the intrinsic conduction velocity transverse to the muscle fiber axis to be two to three times greater in the plane of a muscle layer than perpendicular to it. This would not influence normal cardiac electrical activation, because the endocardial surface of the ventricles is rapidly excited via the Purkinje fiber network, and the radial arrangement of muscle layers will ensure an efficient transmural spread of activation. However, the structural anisotropy of ventricular tissue may well contribute to the patterns of electrical activation associated with various arrhythmias.

A detailed and accurate knowledge of ventricular structure is necessary to understand many aspects of cardiac function. In most analyses of cardiac function, it has been assumed that the material properties of ventricular tissue are transversely isotropic. Our results confirm the belief that ventricular myocardium is a discrete laminar structure in which it is possible to identify three distinct material axes at any point: one in the direction of the muscle fiber axis, a second transverse to the fiber axis in the plane of the muscle layer, and the third perpendicular to that plane. Moreover, we have demonstrated a clear transmural variation in the extent of coupling between adjacent layers. We believe that this information should be incorporated into future quantitative models of cardiac structure.

The authors gratefully acknowledge the expert technical assistance of Lynnette Yep.

This work was supported by project grants from the National Heart Foundation of New Zealand and the Auckland Medical Research Foundation. I. J. LeGrice was funded by the Auckland Medical Research Foundation.

Address for reprint requests: I. J. LeGrice, Dept. of Physiology, School of Medicine, University of Auckland, Private Bag 92019 Auckland, New Zealand.

Received 21 September 1994; accepted in final form 2 March 1995.

REFERENCES

1. **Abrahams, C., J. S. Janicki, and K. T. Weber.** Myocardial hypertrophy in *Macaca fascicularis*: structural remodeling of the collagen matrix. *Lab. Invest.* 56: 676–683, 1987.
2. **Bashey, R. I., A. Martinez-Hernandez, and S. A. Jimenez.** Isolation, characterization and localization of cardiac collagen Type VI: associations with other extracellular matrix components. *Circ. Res.* 70: 1006–1017, 1992.
3. **Cannon, R. O., J. W. Butany, B. M. McMannus, E. Speir, A. B. Kravitz, R. Bolli, and V. J. Ferrans.** Early degradation of collagen after acute myocardial infarction in the rat. *Am. J. Cardiol.* 52: 390–395, 1983.
4. **Caulfield, J. B., and T. K. Borg.** The collagen network of the heart. *Lab. Invest.* 40: 364–372, 1979.
5. **Feneis, H.** Das Gefuge des Herzmuskels bei Systole und Diastole. *Morphol. Jahrb.* 89: 371–406, 1943.
6. **Grimm, A. F., K. V. Katele, and H.-L. Lin.** Fiber bundle direction in the mammalian heart. An extension of the "nested shells" model. *Basic Res. Cardiol.* 71: 381–388, 1976.
7. **Hort, W.** Untersuchungen uber die Muskelfaserdehnung und das Gefuge des Myokards in der rechten Herzkammerwand des Meerschweinchens. *Virchows Arch. Pathol. Anat. Physiol. Klin. Med.* 329: 649–731, 1957.
8. **Hort, W.** Makroskopische und mikrometrische Untersuchungen am Myokard verschieden stark gefullter linker Kammern. *Virchows Arch. Pathol. Anat. Physiol. Klin. Med.* 333: 523–564, 1960.
9. **Hunter, P. J., and B. H. Smaill.** The analysis of cardiac function: a continuum approach. *Prog. Biophys. Mol. Biol.* 52: 101–164, 1988.
10. **Jalil, J. E., C. W. Doering, J. S. Janicki, R. Pick, S. G. Shroff, and K. T. Weber.** Fibrillar collagen and myocardial stiffness in the intact hypertrophied rat left ventricle. *Circ. Res.* 64: 1041–1050, 1989.
11. **Maccallum, J. B.** On the muscular architecture and growth of the ventricles of the heart. *Johns Hopkins Hosp. Rep.* 9: 307–335, 1900.
12. **Mall, F. P.** On the muscular architecture of the ventricles of the human heart. *Am. J. Anat.* 11: 211–266, 1911.
13. **Nielsen, P. M. F., I. J. LeGrice, B. H. Smaill, and P. J. Hunter.** Mathematical model of geometry and fibrous structure of the heart. *Am. J. Physiol.* 260 (*Heart Circ. Physiol.* 29): H1365–H1378, 1991.
14. **Olivetti, G., J. M. Capasso, E. H. Sonnenblick, and P. Anversa.** Side-to-side slippage of myocytes participates in ventricular wall remodeling acutely after myocardial infarction in rats. *Circ. Res.* 67: 23–34, 1990.
15. **Robb, J. S., and R. C. Robb.** The normal heart. Anatomy and physiology of the structural units. *Am. Heart J.* 23: 455–467, 1942.
16. **Robinson, T. F., L. Cohen-Gould, and S. M. Factor.** Skeletal framework of mammalian heart muscle. Arrangement of inter- and pericellular connective tissue structures. *Lab. Invest.* 49: 482–498, 1983.
17. **Robinson, T. F., S. M. Factor, J. M. Capasso, B. A. Wittenberg, O. O. Blumenfeld, and S. Seifter.** Morphology, composi-

tion, and function of struts between cardiac myocytes of rat and hamster. *Cell Tissue Res.* 249: 247–255, 1987.

18. **Robinson, T. F., M. A. Geraci, E. H. Sonnenblick, and S. M. Factor.** Coiled perimysial fibers of papillary muscle in rat heart: morphology, distribution, and changes in configuration. *Circ. Res.* 63: 577–592, 1988.
19. **Smaill, B. H., and P. J. Hunter.** Structure and function of the diastolic heart: material properties of passive myocardium. In: *Theory of Heart: Biomechanics, Biophysics and Nonlinear Dynamics of Cardiac Function*, edited by L. Glass, P. Hunter, and A. McCulloch. New York: Springer-Verlag, 1991, chapt. 1.
20. **Spach, M., and P. C. Dolber.** Relating extracellular potentials and their derivatives to anisotropic propagation at a microscopic level in human cardiac muscle. Evidence for electrical uncoupling of side-to-side fiber connections with increasing age. *Circ. Res.* 58: 356–371, 1986.
21. **Spach, M., P. C. Dolber, and J. F. Heidlage.** Influence of the passive anisotropic properties on directional differences in propagation following modification of the sodium conductance in human atrial muscle: a model of reentry based on anisotropic discontinuous propagation. *Circ. Res.* 62: 811–832, 1988.
22. **Spotnitz, H. M., W. D. Spotnitz, T. S. Cottrell, D. Spiro, and E. H. Sonnenblick.** Cellular basis for volume related wall thickness changes in the rat left ventricle. *J. Mol. Cell. Cardiol.* 6: 317–331, 1974.
23. **Streeter, D. D., Jr., and D. L. Bassett.** An engineering analysis of myocardial fiber orientation in pig's left ventricle in systole. *Anat. Rec.* 155: 503–511, 1966.
24. **Streeter, D. D., Jr., H. M. Spotnitz, D. P. Patel, J. Ross, Jr.,and E. H. Sonnenblick.** Fiber orientation in the canine left ventricle during diastole and systole. *Circ. Res.* 24: 339–347, 1969.
25. **Waldman, L. K., Y. C. Fung, and J. M. Covell.** Transmural myocardial deformation in canine left ventricle. *Circ. Res.* 57: 152–163, 1985.
26. **Weber, K. T., J. S. Janicki, S. G. Shroff, R. Pick, R. M. Chen, and R. I. Bashey.** Collagen remodeling of the pressure-overloaded, hypertrophied nonhuman primate myocardium. *Circ. Res.* 62: 757–765, 1988.
27. **Weber, K. T., Y. Sun, S. C. Tyagi, and J. P. M. Cleutjens.** Collagen network of the myocardium: function, structural remodelling and regulatory mechanisms. *J. Mol. Cell. Cardiol.* 26: 279–292, 1994.
28. **Weisman, H. F., D. E. Bush, J. A. Mannisi, M. L. Weisfeldt, and B. Healy.** Cellular mechanisms of myocardial infarct expansion. *Circulation* 78: 186–201, 1988.
29. **Weitz, G.** Uber das unterschiedliche Verhalten der Lage der Herzmuskelfasern in kontrahiertem und dilatierem Zustand. *Med. Klin. Munich* 46: 1031–1032, 1951.
30. **Wheeler, E. E., J. B. Gavin, and R. N. Seelye.** Freeze-drying from tertiary butanol in the preparation of endocardium for scanning electron microscopy. *Stain Technol.* 50: 331–337, 1975.
31. **Zhao, M., H. Zhang, T. F. Robinson, S. M. Factor, E. H. Sonnenblick, and C. Eng.** Profound structural alterations of the extracellular collagen matrix in postischemic dysfunctional ("stunned") but viable myocardium. *J. Am. Coll. Cardiol.* 10: 1322–1334, 1987.